

Correlated scattering of protons impinging as hydrogen molecules

Jene Golovchenko* and Erik Laegsgaard

Institute of Physics, University of Aarhus, Denmark

(Received 20 July 1973)

The joint energy and angular-distribution function of protons transmitted through a thin foil when incident as 2-MeV H_2^+ has been measured. The experimental result is compared with simple calculations and satisfactory agreement is obtained.

In the past few years several workers have reported observing manifestations of molecular binding in scattering experiments with incident molecules of hydrogen. Bacher *et al.*¹ saw such effects on the 14.2-MeV $^{12}C(p, p) ^{12}C$ resonance. Caywood *et al.*² and Eisen *et al.*³ showed modification of channeling backscatter results, while Poizat *et al.*⁴ observed H_2^+ molecules emerging from a thin foil. Finally, Stotterfoht *et al.*⁵ observed a difference in the fluorescence yield of the argon L shell with incident protons and H_2^+ .

In recent experiments we have observed protons transmitted through thin self-supporting carbon foils when the incident particles were either 2-MeV H_2^+ or 1-MeV H^+ ions, with the motivation of measuring physical phenomena depending upon the correlation of proton positions provided by the binding in the initial hydrogen molecular ions. Our preliminary findings show that the energy and angular distributions of such transmitted protons have a strong dependence upon this correlation. Advantage may be taken of these effects to study proton pairs of a given alignment within the solid. Indeed even the individual spatial identities may be determined. With such capabilities, interesting new approaches towards measuring the interaction of atomic systems become available. In particular, we discuss inelastic excitation of the solid and show that effects due to correlation may be expected.

I. EXPERIMENTAL PROCEDURE

The experimental setup used mass-analyzed ions provided by the Aarhus University 2-MeV Van de Graaff facility; incident beam energy fluctuations were less than 1 keV; the incident particles were collimated to less than 5×10^{-4} rad angular full width at half-maximum (FWHM), and the beam-spot size on the sample was ~ 0.1 mm. It will be seen shortly that such fine collimation is essential for these measurements. Directly behind the thin-carbon sample, a small electromagnet swept (at 10 Hz) the dispersed transmitted protons in a horizontal plane across a 0.1-mm collimator,

500 mm behind the sample. In this way, any representative part of the final angular distribution could be selected for further study. This magnet needed only to supply a maximum deflection of 5×10^{-3} rad for our measurements. Those particles transmitted through the final collimator were energy analyzed in the vertical plane by a magnetic spectrometer with a 40-mm-long position-sensitive solid-state detector⁶ in its focal plane. The magnet dispersion ($\Delta X = 800 \text{ mm} \cdot \Delta E/E$) and length of the detector allowed the entire energy region of interest to be studied at one time without changing the magnetic field. Energy resolution for 1-MeV protons was ~ 3.1 keV FWHM. Figure 1 provides a schematic illustration of the apparatus and the electronics of the data-taking equipment.

Thus, if the energy spectrum obtained is synchronized with the sweeping magnet current (which is a ramp in time), then joint energy and angular distributions are obtained. In addition all results are normalized consistently, with beam-current fluctuations being averaged out over the course of the measurement (~ 20 min). Those readers familiar with similar kinds of transmission measurements will recognize the important influence normalization problems have in the design of such experiments.

II. EXPERIMENTAL RESULTS

Figure 2 (curve 2) shows the angular distribution of all transmitted protons through an approximately $2\text{-}\mu\text{g}/\text{cm}^2$ carbon foil with an incident beam of 1-MeV H^+ . The width of this distribution is 1.46×10^{-3} rad FWHM and is not well represented by a Gaussian. Also shown in Fig. 2 (curve 3) is the angular distribution of transmitted protons when 2-MeV H_2^+ is incident. A rather large broadening and flattening out of the multiple scattering distribution is observed. For completeness the measured angular divergence of the incident 1-MeV H^+ beam is also shown (curve 1).

Even more dramatically, Fig. 3 shows the more detailed two-dimensionally-displayed joint energy

and angular distribution of the emergent protons with 2-MeV H_2^+ incident. The angle is measured relative to the incident beam direction. For zero angle the energy distribution shows two distinct peaks situated in a roughly symmetrical way about half the incident beam energy. As the angle of observation increases, the peaks appear to merge at $\sim 2.5 \times 10^{-3}$ rad. The angular distribution shows a similar behavior as the energy of observation is changed.

III. DISCUSSION AND ANALYSIS

The main features of the angular-energy distributions for incident H_2^+ may be understood in terms of simple mechanical arguments. As the incident molecule passes through the first few atomic layers of the foil, the electron responsible for the binding is lost by ionization. The two protons then repel one another via a (screened) Coulomb potential. In the two-proton center-of-mass system, 13.6 eV of potential energy transforms into kinetic energy. (An initial proton separation of 1.06 Å is assumed.⁷) This transformation alone results in significant modification of the energy and angular distribution of the beam. For example the proton kinetic energy in the laboratory system, after separation is complete, is

$$E_f = \frac{1}{2} E_{inc} + \frac{1}{2} E_p \pm (E_{inc} E_p - E_{inc}^2 \sin^2 \phi)^{1/2}. \quad (1)$$

Here, E_{inc} is the incident kinetic energy of the molecule, E_p the initial potential energy of the

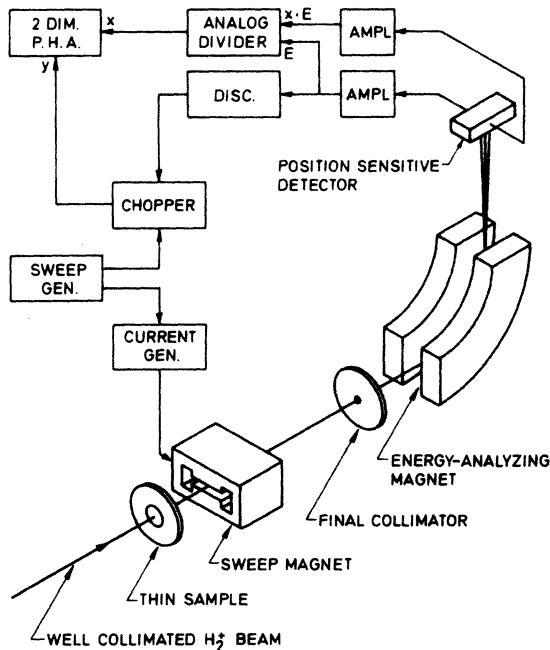


FIG. 1. Schematic illustration of the experiment.

two-proton system and ϕ is the angle of observation in the laboratory relative to the incident beam direction. (For the interested reader the mathematical details of this problem may be found in the Appendix.) It may be noted that just upon leaving the foil, the proton separation has increased by $\sim 10\%$ over the initial value. Thus most of the repulsion occurs after the foil.

For our experiments, with 2-MeV H_2^+ at $\phi = 0$, we expect to detect protons of energy 1.0052 and 0.9948 MeV corresponding to protons that break up aligned with the beam direction. (We neglect the small energy loss due to excitation of electrons in the foil.) The higher-energy proton comes from the front position and the lower-energy proton from the back. As the angle ϕ is increased, these two energies merge towards one another until finally they meet at 1.000 MeV, corresponding to protons breaking up perpendicular to the incident beam direction. Here

$$\phi = \phi_{max} = (E_p/E_{inc})^{1/2}. \quad (2)$$

Also assuming the molecular orientation to be isotropic, we find, for the probability per unit solid angle for detecting a proton with $\phi \leq \phi_{max} \ll 1$,

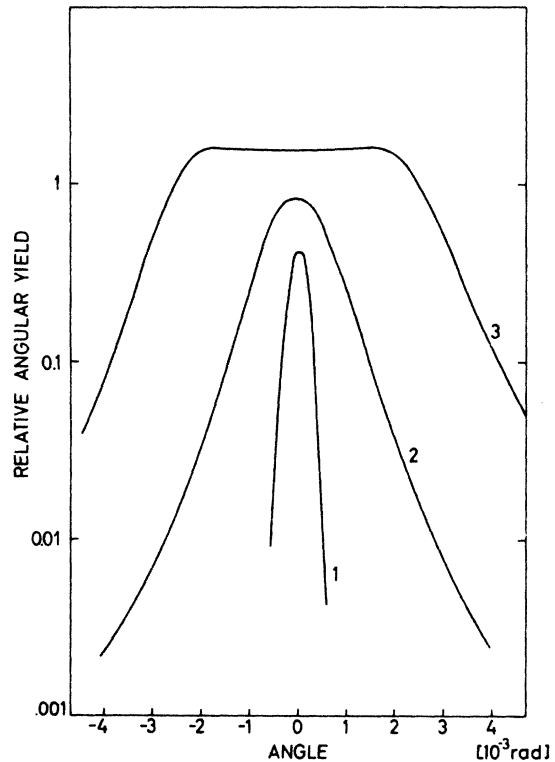


FIG. 2. (1) Angular distribution of the incident beam. (2) Angular distribution of the H^+ beam after passing the foil. (3) H_2^+ angular distribution after passing through the foil.

$$f(\phi) = \frac{1}{2\pi} \frac{E_{\text{inc}}}{E_p} \left(1 - \frac{E_{\text{inc}}}{E_p} \phi^2\right)^{-1/2}. \quad (3)$$

But, alas, all is not so simple. Deviations from the ideal behavior already discussed may result from three causes. Most interesting in these measurements, although least important, is the modification caused by uncertainty in relative position between protons associated with the quantum-mechanical description of the H_2^+ molecule. For an incident particle in the ground state, this effect produces about a 600-eV spread in the energy spectrum obtained at $\phi = 0$. (The uncertainty in momentum produces a much smaller effect.) Multiple scattering in the foil and experimental energy resolution completely overwhelm this effect. We have calculated the energy and angular distributions (details are in the Appendix) including multiple scattering and energy resolution as measured from the H^+ incident case. Figure 4 shows the relative contribution from these effects to the $\phi = 0$ case. The agreement with the experimental points is deemed quite acceptable. Note should be taken of the fact that the H^+ multiple scattering distribution is not of a Gaussian type. This is to be expected for such thin foils. The distribution can be represented quite accurately for angles up to ϕ_{max} by a sum of two Gaussians, one having a FWHM of 1.47×10^{-3} rad and a weight of $\frac{4}{5}$, the other having twice this width and a weight of $\frac{1}{5}$. This distribution was used in obtaining the result in Fig. 4. We are not aware of any theoretical estimates that may be compared with this distribution (in this experiment Bohr's parameter $\kappa = Z_1 Z_2 e^2 / \hbar v \approx 1$).

Finally, an interesting, though somewhat speculative, application of the above technique may be to study the effect of proton correlation on the inelastic excitation of the solid. It is well known that perturbation treatments of energy loss of

fast particles in matter show a proportional dependence on the square of the charge of the penetrating particle. Thus, as the separation between two protons varies from zero to some large value, the energy-loss rate per proton may be expected to change by a factor of 2. A convenient, though perhaps crude, model for estimating the detailed dependence on proton separation and orientation is that of particles penetrating through a free-electron gas. Calculations in the linear dielectric-response approximation indicate that, for some orientations and a particle separation of two Bohr radii, one may expect from distant collisions alone a 50% increase in the average energy-loss rate per particle, compared with only a single penetrating proton. Details of these calculations will be reported later.

Experimental attempts to verify this effect in a quantitative manner have been frustrated by the small energy loss observed in the measurements (~ 500 eV). We hope to be able to clear up this matter in the not too distant future.

Deepest appreciation for guidance and criticism during the course of this work is due J. U. Andersen, J. Lindhard, and H. H. Andersen. One of us (JG) would like to express his thanks to the Aarhus University, Institute of Physics, for the privilege and pleasure of being a guest.

APPENDIX

Consider a fast incident H_2^+ molecule. Neglecting the contribution from rotations and vibrations, the incident kinetic energy is

$$E_{\text{inc}} = M_p v_{\text{inc}}^2,$$

where v_{inc} is the incident proton velocity and M_p the proton mass. Assuming that the binding electron is ionized and no longer effects the proton, motions of repulsion occur, resulting in a final

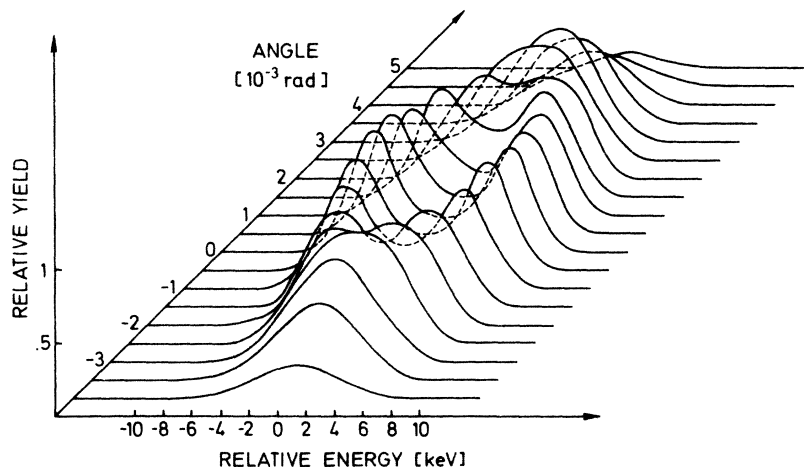


FIG. 3. Joint angle-energy distribution. Energy is measured relative to 1 MeV.

kinetic energy per proton of

$$E_f = \frac{1}{2} M_p (\vec{v}_{inc} + \vec{v}_p)^2 \\ = \frac{1}{2} E_{inc} + \frac{1}{2} E_p + (E_{inc} E_p)^{1/2} \cos \theta .$$

Here θ is the polar angle determined by the molecular orientation relative to the incident beam direction, and E_p is the initial potential energy of the repelling protons, i.e.,

$$E_p = M_p v_p^2 = e^2 / r_{12} ,$$

where $r_{12} = 1.06 \text{ \AA}$ is the average distance between the protons in a H_2^+ molecule. The final polar angle ϕ in the laboratory at which the proton will be detected is determined from

$$\tan \phi = v_p \sin \theta / (v_{inc} + v_p \cos \theta) .$$

Since in this work $v_{inc} \gg v_p$, we have

$$\phi = (E_p / E_{inc})^{1/2} \sin \theta = \phi_{max} \sin \theta .$$

Such a small angle approximation is assumed hereafter.

Consider $C(\phi, E_f, E_p)$, the normalized joint final angle and energy distribution resulting from an initially uniform spherical distribution for the H_2^+ molecule. Introducing dimensionless variables

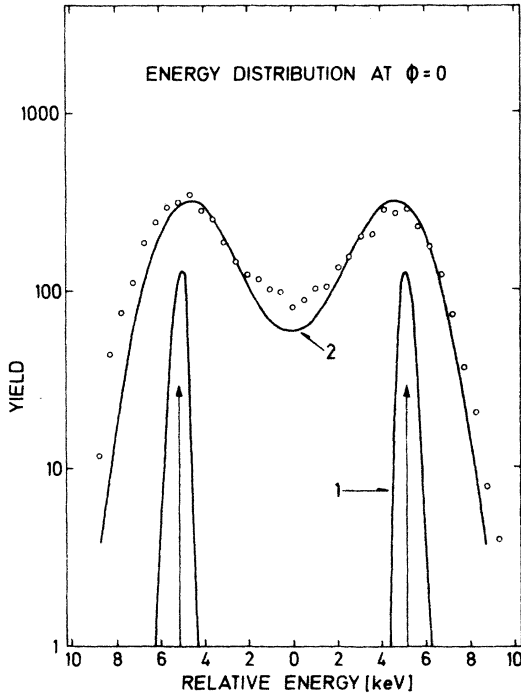


FIG. 4. Comparison of experimental and calculated distributions for $\phi = 0$. \circ : experimental points; 1: distribution with zero point motion; 2: calculated distribution taking into account two-component multiple scattering and energy resolution as observed for 1-MeV H^+ on the same target foil.

$$\Phi = \phi / \phi_{max} ,$$

$$\xi = (E_f - \frac{1}{2} E_{inc} - \frac{1}{2} E_p) / (E_{inc} E_p)^{1/2}$$

with differential solid angles

$$d\Omega = \Phi d\Phi d\chi = \phi d\phi d\chi / \phi_{max}^2 = d\omega / \phi_{max}^2 ,$$

we have

$$C(\phi, E_f, E_p) d\omega dE_f \\ = d\Omega d\xi \frac{1}{4\pi\Phi} \int_{-1}^1 d(\cos\theta) \delta(\Phi - \sin\theta) \delta(\xi - \cos\theta)$$

if $\Phi \leq 1$, while for $\Phi > 1$, C is zero. χ is the angle measuring the azimuthal orientation of the molecule.

Using C , other distribution functions of interest may be easily determined. For example, the integral energy distribution is

$$A(E_f, E_p) dE_f \equiv dE_f \int d\omega C = \frac{1}{2} d\xi, \quad |\xi| \leq 1 , \\ = 0, \quad |\xi| > 1 .$$

Similarly, the integral angular distribution is given by

$$B(\phi, E_p) d\omega \equiv d\omega \int dE_f C = \frac{1}{2\pi} (1 - \Phi^2)^{-1/2} d\Omega, \quad \Phi \leq 1 , \\ = 0, \quad \Phi > 1 .$$

In order to represent the effect of multiple scattering in the foil on the final results, consider the "folding" of a Gaussian angular-distribution function with C . Thus, let

$$D(\phi, E_f, E_p) d\omega dE_f = d\omega dE_f \int d\omega' C(\phi', E_f, E_p) M(K) .$$

Here

$$M(K) = \frac{1}{\pi(\alpha\phi_{max})^2} \exp\left(-\frac{K^2}{(\alpha\phi_{max})^2}\right) ,$$

and

$$K^2 = \phi^2 - 2\phi\phi' \cos\chi' + \phi'^2 ,$$

where α measures the dimensionless angular extension of the multiple scattering in the foil. One then finds for each component Gaussian term

$$D(\phi, E_f, E_p) d\omega dE_f = \frac{1}{2\pi\alpha^2} \exp\left(-\frac{\Phi^2 + 1 - \xi^2}{\alpha^2}\right) \\ \times I_0\left(\frac{2\Phi}{\alpha^2} (1 - \xi^2)^{1/2}\right) d\Omega d\xi, \quad |\xi| \leq 1 , \\ = 0, \quad |\xi| > 1 ,$$

where I_0 is a modified Bessel function. With D one may now fold a Gaussian distribution to account

for the energy resolution of the particle-detection system, i.e.,

$$N = \frac{1}{\sqrt{\pi}} \epsilon (E_{\text{inc}} E_p)^{1/2} \exp\left(-\frac{(E_f - E_i)^2}{\epsilon^2 E_{\text{inc}} E_p}\right),$$

with ϵ being a dimensionless measure of the energy resolution. If the argument of the modified Bessel function is quite small ($\Phi \approx 0$), this program may be carried to completion analytically, giving

$$\begin{aligned} F(\phi, E_f, E_p) d\omega dE_f \\ = \frac{1}{4\pi\alpha(\alpha^2 - \epsilon^2)^{1/2}} \exp\left(+\frac{b^2 - ac}{a}\right) \\ \times \left[\operatorname{erf}\left(\frac{b}{\sqrt{a}} + \sqrt{a}\right) - \operatorname{erf}\left(\frac{b}{\sqrt{a}} - \sqrt{a}\right) \right] d\Omega d\xi \end{aligned}$$

for $a \neq 0$. Here

$$a = \frac{1}{\epsilon^2} - \frac{1}{\alpha^2}, \quad b = -\frac{\xi}{\epsilon^2}, \quad c = \frac{\xi^2}{\epsilon^2}.$$

For $\Phi \neq 0$ we have resorted to numerical methods to determine F . The calculated results shown in

Fig. 4 have been obtained with the above considerations in mind.

For the sake of completeness, the energy angle distribution may be calculated including only the effect of zero-point motion of the incident molecule (assumed to be in a harmonic oscillator ground state). For this purpose the distribution of E_p should be calculated and folded with C . The result is

$$\begin{aligned} H(\phi, E_f) d\omega dE_f = \frac{1}{2\pi^{3/2}} (\xi^2 + \Phi^2)^{-5/2} \\ \times \Gamma \exp\left(-\Gamma^2 \frac{1 - (\xi^2 + \Phi^2)}{\xi^2 + \Phi^2}\right) d\Omega d\xi, \end{aligned}$$

where

$$\Gamma = (\hbar\omega_H \frac{1}{2} M_p v_0^2 / E_p^2)^{1/2}.$$

$\hbar\omega_H$ is the distance between oscillator energy levels, and $\frac{1}{2}M_p v_0^2$ is the kinetic energy of a proton at the Bohr velocity. This result is also plotted in Fig. 4 for $\Phi = 0$.

*Present address: Physics Department, Brookhaven National Laboratory, Upton, New York 11973.

¹A. D. Bacher, E. A. McClatchie, M. S. Zisman, T. A. Weaver, and T. A. Tombrello, Nucl. Phys. A **181**, 453 (1972).

²J. M. Caywood, T. A. Tombrello, and T. A. Weaver, Phys. Lett. **37**, 350 (1971).

³F. H. Eisen and E. Uggerhøj, Radiat. Eff. **12**, 233 (1972).

⁴J. C. Poizat and J. Remillieux, J. Phys. B **5**, 94 (1972).

⁵N. Stolterfoht, F. J. de Heer, and J. Van Eck, Phys. Rev. Lett. **30**, 1159 (1973).

⁶E. Laegsgård, F. W. Martin, and W. M. Gibson, IEEE Trans. Nucl. Sci. NS-15, No. 3, 239 (1968).

⁷G. Herzberg, *Molecular Spectra and Molecular Structure* (Prentice-Hall, New York, 1939).